

## Changes in the Total Number of Dentate Granule Cells in Juvenile and Adult Rats: A Correlated Volumetric and <sup>3</sup>H-Thymidine Autoradiographic Study\*

S. A. Bayer

Laboratory of Developmental Neurobiology, Dept. of Biological Sciences, Purdue University, West Lafayette, IN 47907, USA

**Summary.** The total number of granule cells in the dentate gyrus was estimated in 17 male rats, four each aged 30, 120, and 200 days, and five aged 365 days. There is a substantial 35–43% linear increase between 1 month and 1 year. Two parameters of the granular layer are involved in the numerical change. First, total granular layer volume grows linearly with age. Second, average volume of a single granule cell nucleus in the ventral dentate gyrus decreases with age. Older rats tend to have a larger granular layer filled with more and smaller cells. In another group of 21 male rats, <sup>3</sup>H-thymidine injections were given on four consecutive days during juvenile (30–33, n = 6) and adult life (60–63, n = 5; 120–123, n = 6; 180–183, n = 4). All animals survived to 200 days of age. The proportion of labeled mature granule cells and labeled presumptive granule cell precursors were determined in anatomically-matched slices. With older ages at injection, there is a decline in labeled mature granule cells and a concurrent increase in labeled precursors. These data are compatible with the constant level of granule cell increase determined volumetrically. Most of the late granule cells originate nearly simultaneously along the base of the main bulk of the granular layer; very few are found in the dorsal tip (septal extreme) and ventral tip (temporal extreme). This study is the first demonstration of a net numerical gain in a neuronal population during adulthood in the mammalian brain. Since the granule cells play a pivotal role in hippocampal function, these data suggest that their influence grows with age.

**Key words:** Rat – Dentate granule cells – Volumetric analysis – Adult – Neurogenesis

### Introduction

Since Altman's study (1963), it has been repeatedly shown with <sup>3</sup>H-thymidine autoradiography that dentate granule cells in the hippocampus continue to be produced during the adult period in rats (Altman and Das 1965, 1966; Bayer 1976; Kaplan and Hinds 1977). It was not known whether these new neurons add to the population or replace those that die during adult life. Several years ago, Bayer and Altman (1975) obtained circumstantial evidence that the number of granule cells was increasing up to 120 days of age in the rat. Therefore, the present study was designed to systematically determine numerical age changes in the granule cell population, and to correlate these changes with levels of neurogenesis during the juvenile and adult period.

### Methods

#### *Volumetric Analysis*

The total number of granule cells was estimated in 17 Purdue-Wistar male rats, four each aged 30, 120, and 200 days, and five aged 365 days. The animals were killed with a double transcardial perfusion first with 10% neutral formalin (10 min) followed by Bouin's fixative (5 min). The brains were stored in 10% neutral formalin until the block containing the entire right hippocampus was embedded in methacrylate (Polysciences, Inc.). Serial 3 μm slices were cut in the horizontal plane using steel knives on a JB-4 microtome (Sorvall) and were stained with cresyl violet. Care was taken to see that the slices were of uniform thickness.

Two previous volumetric estimates of granule cell numbers in rats employed modified Abercrombie (1946) correction factors to counts of neuronal nucleoli (Schlessinger et al. 1975; Gaarksjaer 1978). This method was unworkable in our preparations since the Purdue-Wistar strain consistently shows double nucleolus-like bodies in many granule cell nuclei (arrow in Fig. 1C). Consequently, the nucleus was chosen as the cell structure to be quantified. The method (Puri and Yackel 1981) was based on the equation:

$$N = V_t / V_n,$$

\* Supported by the National Science Foundation (Grant No. BNS 79-21303)

Offprint requests to: S. A. Bayer, PhD (address see above)

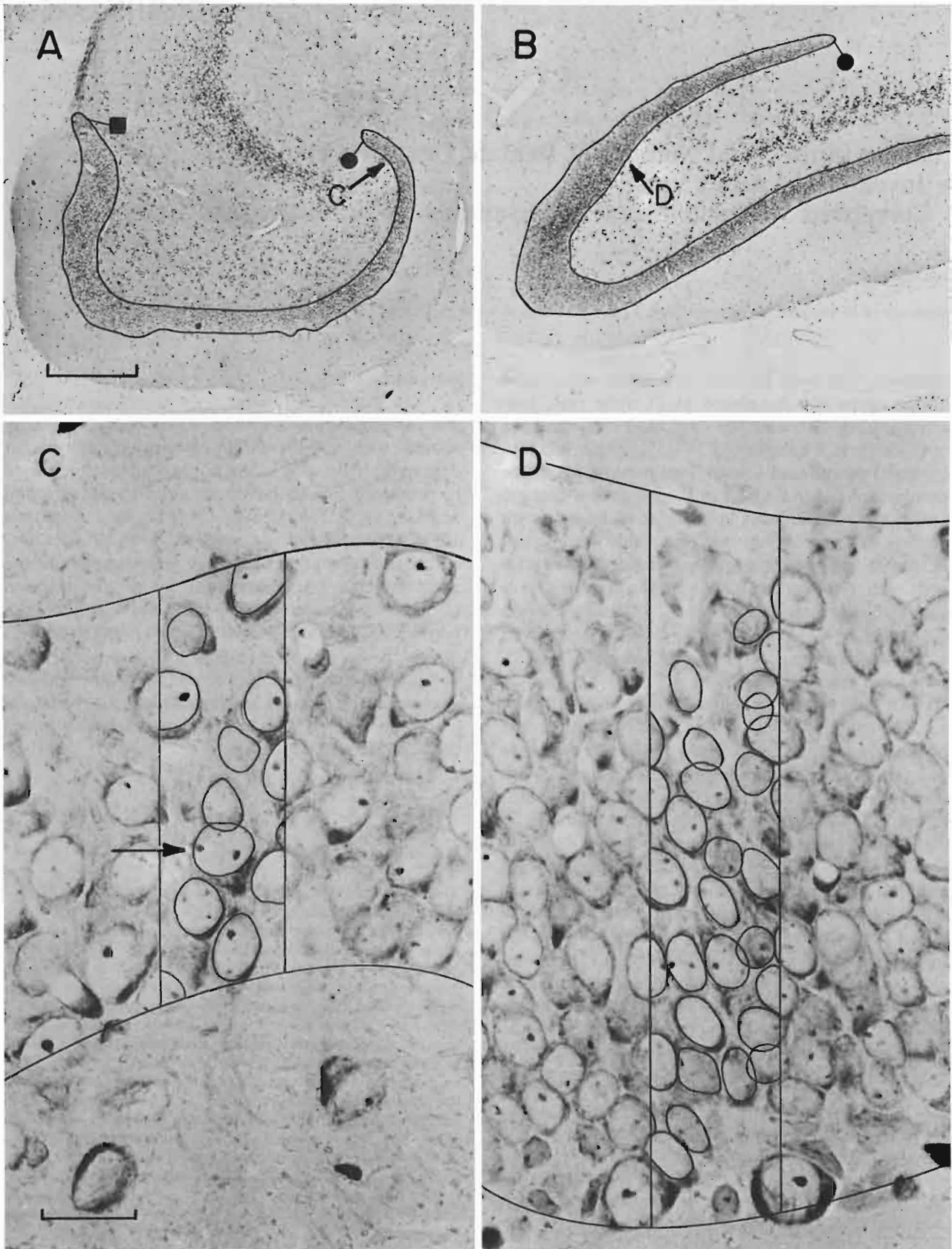


Fig. 1A-D

where  $N$  is the total number of cells;  $V_t$  is the total volume of all granule cell nuclei, and  $V_a$  is the average volume of an individual granule cell nucleus. Both  $V_t$  and  $V_a$  were estimated with statistical techniques, and the equation was solved for  $N$ . A detailed description of the procedures used is provided in the appendix. Briefly, we experimentally determined  $V_t$  using low magnification photomicrographs of ventral (Fig. 1A) and dorsal (Fig. 1B) granular layer slices at regularly spaced intervals. The granular layer was divided into 25  $\mu\text{m}$  wide strips running perpendicular to the length; each strip was considered as a possible sample. We randomly chose 200 strips from the total pool in all selected slices for examination at high magnification (Fig. 1C, D). For each slice that was examined, the area of the granular layer, areas of each selected sample, and areas of all complete and partial granule cell nuclear profiles (outlined in Fig. 1C, D) within the samples were measured with a Summagraphics digitizer interfaced to a Wang 2200 computer (accuracy was within 0.75). These measurements provided the basis for the final estimation of  $V_t$ .

To estimate average granule cell nuclear volume ( $V_a$ ) in the ventral part of the granular layer, for example, the nuclear profiles completely contained in all ventral samples (between 700–1,000 in each animal) were used to form empirical distributions of observed ventral granule cell nuclear sizes. Complete profiles contained in all dorsal samples (usually 2,000 or more observations for each animal) were similarly processed. Average nuclear volume in both parts was estimated by applying the method of Hendry (1976) to the empirical distributions.

In order to minimize measuring error trends within age groups, the first four animals processed contained one member from each group, the next four contained a second member, and so on, until all the analyses were completed. The error involved in outlining the nuclear profiles within the samples was also determined. After the last animal was completed, the number of cells in the ventral part of the granular layer in the first animal measured was recalculated. A duplicate set of high magnification photographs of each sample was printed, the samples were relocated in the microscopic field, and granule cell nuclear profiles were outlined. Both  $V_t$  and  $V_a$  were reestimated using the second set of photographs. There was a 4.5% numerical increase in the second set of data; this was mainly due to the later use of improved microscopic eyepieces which were not initially available. The amount of computer operator error in digitizing nuclear profile and sample areas was determined by remeasuring all areas in the dorsal part of the granular layer in one of the animals (using different operators) and recalculating the number of cells; there was a 0.75% difference between the two sets of data.

#### <sup>3</sup>H-thymidine Autoradiographic Analysis of Juvenile and Adult Granule Cell Neurogenesis

The proportion of labeled mature granule cells and precursor cells to total cells was determined in groups of Purdue-Wistar male rats after four consecutive daily injections of <sup>3</sup>H-thymidine according to the following schedules: 30–33d ( $N = 6$ ), 60–63d ( $N = 5$ ), 120–123d ( $N = 6$ ), and 180–183d ( $N = 4$ ). All animals survived to

postnatal day 200 when they were transcardially perfused with 10% neutral formalin. The brains were placed in Bouin's fixative for 24 h then were stored in 10% neutral formalin until they were embedded in paraffin. Serial 6  $\mu\text{m}$  slices were cut in the sagittal plane (every 15th slice was saved); slides were dipped in Kodak NTB-3 emulsion, exposed for 3 months, developed in Kodak D19, and were poststained with hematoxylin and eosin. Anatomically matched slices were selected for cell counts of the medial tip of the dorsal dentate gyrus (septal extreme), medial tip of the ventral dentate gyrus (temporal extreme), 1.0 mm lateral to the midline (septal level), and 3.6 mm lateral to the midline (temporal level). The number of labeled and unlabeled mature granule cells was determined (obvious glial and endothelial cells were eliminated) and the proportion of labeled cells was calculated. Small cells (some of which may be glia) either immediately below the granular layer or embedded into the base were also classed as either labeled or unlabeled, and the proportion of labeled cells was calculated. The analysis of variance was applied to the data to test for age-related changes. The sign test (Conover 1971) was used to analyze trends in cell labeling within individual animals; the rationale for the use of this statistic is provided elsewhere (Bayer 1980).

## Results

### Volumetric Analysis

The total number of dentate granule cells in the right hippocampus is plotted in Fig. 2A. The mean of the 30 day age group was  $894,146 \pm 30,969$ , that at 120 days was  $978,090 \pm 59,278$ , that at 200 days was  $1,107,717 \pm 61,854$ , and that at 1 year was  $1,276,734 \pm 37,235$ . Error bounds on the final estimate for each animal ranged from 33,635 to 63,336. Between 1 month and 1 year, there is a 43% gain in cell number which the analysis of variance showed to be primarily due to age differences ( $F = 34.16$ ,  $p < 0.0001$ ). There is a high positive correlation with age and cell number (Pearson  $r = 0.86$ ,  $p < 0.0001$ ). Regression analysis shows a significant linear increase with age (solid line, Fig. 2A;  $F = 38.93$ ,  $p < 0.0001$ ), and cells are added at the approximate rate of 1,149/day between 30 and 365 days. Assuming that the left hippocampus has similar gains, nearly 770,000 granule cells originate between 1 month and 1 year.

At 365 days, one of the animals had an abnormal total cell count which was 4.73 standard deviations below the mean of the other four animals (161, Fig. 2A). When this animal is included, the mean at 1 year drops to  $1,206,209 \pm 76,194$  and there is a

**Fig. 1A–D.** The dentate granular layer in a 30 day old rat. **A** and **B** are low magnification (Bar = 0.4 mm) views of the area of the granular layer ( $A_g$ ) in horizontal slices of ventral (**A**) and dorsal (**B**) parts; only the posterior portion of the granular layer is shown in **B**. The length at the base of the layer was measured starting with the tip of the ectal limb (circle) and ending with the tip of the endal limb (square) to determine the total number of available samples ( $N_i$ , see Appendix). **C** and **D** are high magnification (Bar = 20  $\mu\text{m}$ ) views of samples randomly drawn from these ventral (**C**, indicated by arrow in **A**) and dorsal (**D**, indicated by arrow in **B**) slices. Complete and partial granule cell nuclear profiles are outlined within each of the sample areas. Arrow in **C** indicates a granule cell with two nucleolus-like bodies. Notice that the profiles in **C** tend to be slightly larger than those in **D**. (3  $\mu\text{m}$  methacrylate slices stained with cresyl violet)

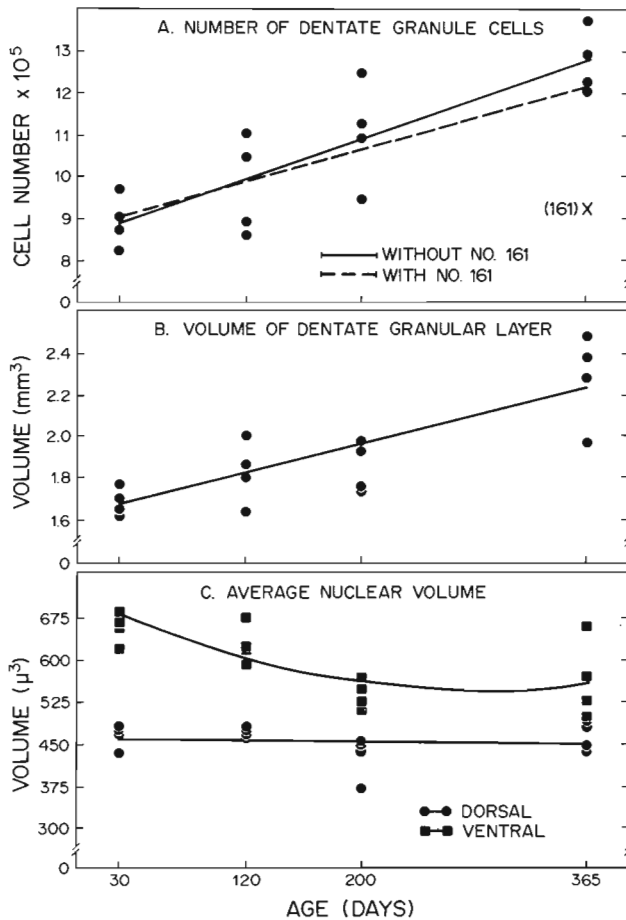


Fig. 2. Scattergrams with regression lines of best fit showing total number of dentate granule cells (A), total volume of the dentate granular layer (B), and average nuclear volume in dorsal and ventral parts of the granular layer (C) in the right hippocampus.

35% gain between 1 month and 1 year (dashed line, Fig. 2A; analysis of variance,  $F = 14.66$ ,  $p < 0.0021$ ; Pearson  $r = 0.72$ ,  $p < 0.001$ ; regression analysis,  $F = 16.22$ ,  $p < 0.001$ ). Since this animal is not representative of the 1 year age group, it was eliminated from the data shown in Fig. 2B, C.

The volume of the right hippocampal dentate granular layer is plotted in Fig. 2B. There is a 35% increase between 30 and 365 days which is primarily due to age (analysis of variance,  $F = 25.68$ ,  $p < 0.0003$ ). Regression analysis shows these data to be linear ( $F = 25.61$ ,  $p < 0.0001$ ) with a positive correlation between age and total volume (Pearson  $r = 0.80$ ).

The average granule cell nuclear volumes in ventral and dorsal parts of the granular layer are depicted in Fig. 2C. In the ventral part, there is an 18% decrease between 30 and 365 days (analysis of variance,  $F = 7.77$ ,  $p < 0.0038$ ). Regression analysis

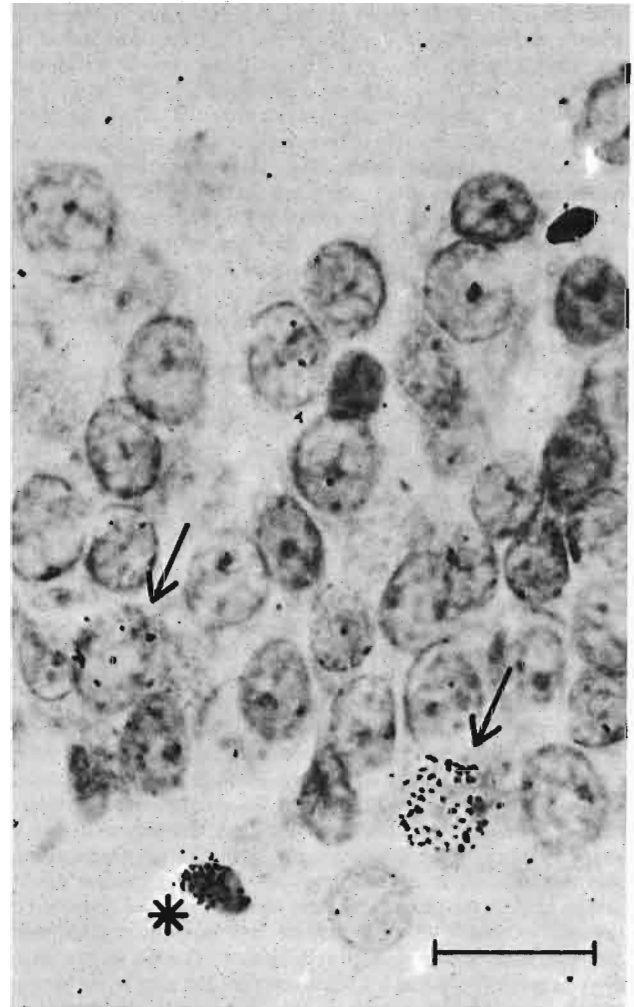


Fig. 3. Labeled mature granule cells (arrows) and a labeled presumptive granule cell precursor (asterisk) in the granular layer endal limb in a rat given four injections of  $^3\text{H}$ -thymidine on 120–123 days of age and killed on 200 days of age.

show these data to be primarily linear ( $F = 9.63$ ,  $p < 0.008$ ) with a negative correlation between age and cell volume (Pearson  $r = -0.64$ ). There is also a significant quadratic term in these data ( $F = 5.74$ ,  $p < 0.0356$ ):

$$y = 706 - 1.12x + 0.0012x^2,$$

where  $y$  is predicted volume and  $x$  is age. The quadratic regression curve is given in Fig. 2C. Overall, the packing density increases from 448,808 cells/mm<sup>3</sup> at 30 days, peaks at 508,581 cells/mm<sup>3</sup> on 200 days, and declines slightly to 500,636 cells/mm<sup>3</sup> at 355 days. Cell volume in the dorsal part is considerably smaller in all animals (sign test,  $p < 0.0001$ ) and does not change across age groups. Due to the

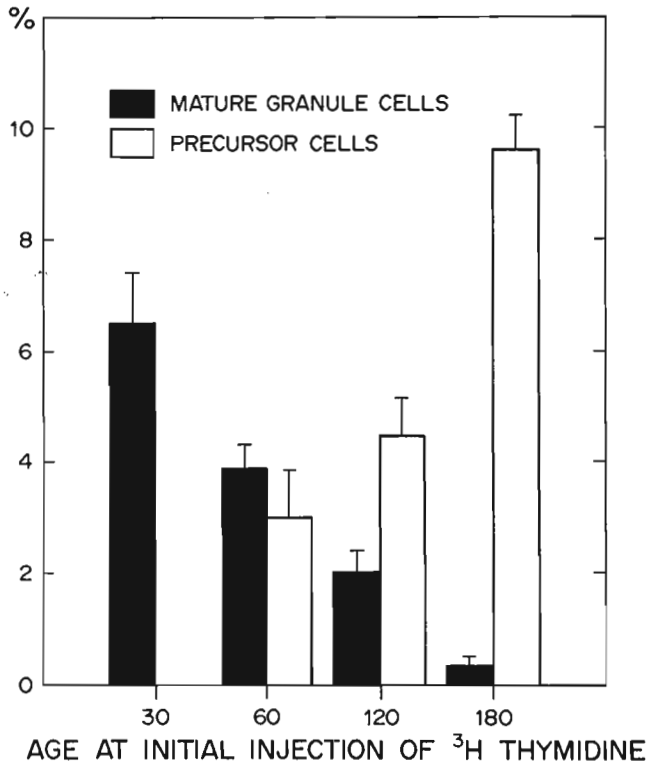


Fig. 4. Means (with standard deviations) of the proportion (labeled cells to total cells) of labeled mature granule cells (black bars) and labeled presumptive precursor cells (white bars) in animals aged 200 days after four consecutive daily injections of <sup>3</sup>H-thymidine began of the days indicated. These data were collected from eight sagittal slices of the granular layer, four each at 1.0 mm and 3.8 mm lateral to the midline

smaller cell size, packing density is higher in the dorsal than in the ventral part (approximately 641,000 cells/mm<sup>3</sup>).

*Analysis of Juvenile and Adult Granule Cell Neurogenesis*

Mature dentate granule cells were routinely labeled after injections of <sup>3</sup>H-thymidine in juvenile and adult rats (arrows, Fig. 3) as well as small cells lying beneath the granular layer (asterisk, Fig. 3) and embedded into the base. There is evidence that some of these small cells, which cannot be distinguished from glia in paraffin sections, are granule cell precursors (Altman and Das 1966; Bayer and Altman 1974; Schlessinger et al. 1975), and mitotic figures have been occasionally observed in this zone in adult animals (Bayer, unpubl. observ.). The proportion of labeled granule and precursor cells was determined in eight sagittal slices, four each at 1.0 and 3.6 mm lateral to the midline. Figure 4 shows that the

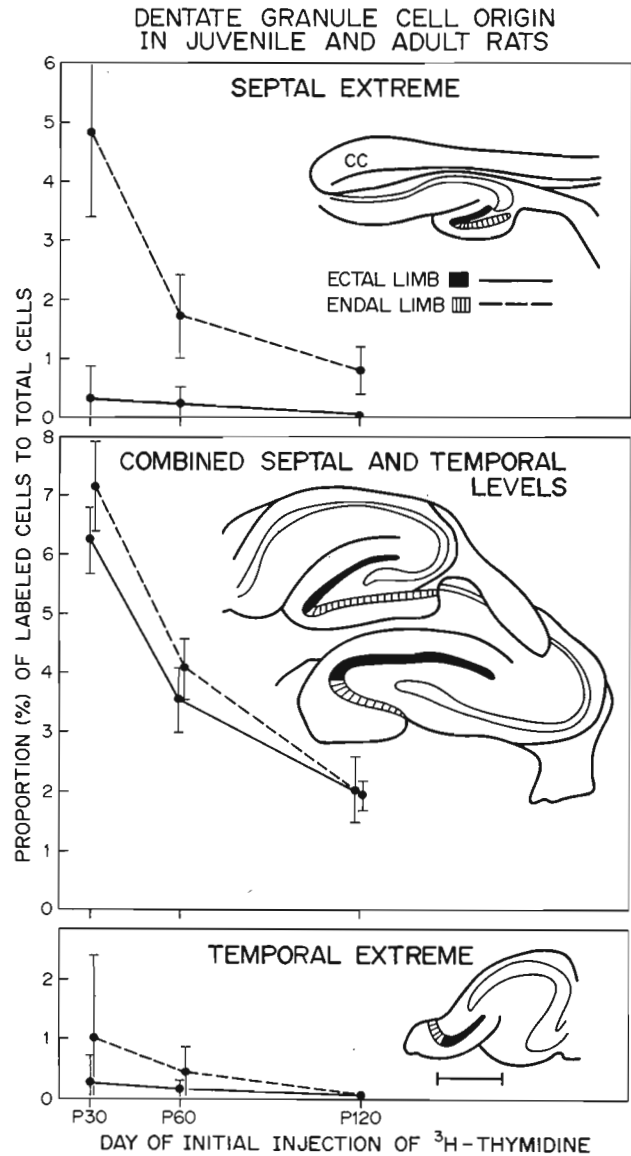


Fig. 5. The mean ratio (with standard deviation) of labeled mature granule cells to total cells in the ectal (solid black, solid line) and endal (stripes, dashed line) limbs of the granular layer at four sagittal levels (Bar = 1.0 mm)

proportion of labeled mature granule cells decreases linearly with age (analysis of variance,  $F = 621.54$ ,  $p < 0.00001$ ) while, at the same time, the proportion of labeled precursor cells increases linearly (analysis of variance  $F = 167.55$ ,  $p < 0.00001$ ). The proportion of labeled precursor cells was not quantified in animals injected on 30–33 days because some glial generation is still taking place at this time (Bayer and Altman 1975).

Gradients of neurogenesis in the mature granule cell population were further investigated at four anatomically matched levels in the sagittal plane

(drawings, Fig. 5). At each level, the ectal (facing CA1) and endal (facing the thalamus) limbs were quantified separately. The sign test showed that granule cell neurogenesis at the septal and temporal levels was not significantly different so the data were combined in the middle graph, Fig. 5. Granule cell neurogenesis in the septal and temporal extremes is significantly lower ( $p < 0.0001$ ) than in the combined septal and temporal levels. The endal limb has more neurogenesis than the ectal limb at the septal extreme ( $p < 0.0001$ ) and at the combined septal and temporal levels ( $p < 0.013$ ), but not at the temporal extreme, where granule cell neurogenesis was virtually nonexistent. Neurogenetic gradients in labelled mature granule cells were not quantified in animals injected in 180–183 days because the short survival time did not allow a representative number of cells to differentiate from the labeled precursors.

## Discussion

### *Comments on the Volumetric Analysis*

By keeping the number of samples analyzed at 200 for each animal, the error of the estimate for the total number of granule cells (see Appendix) was controlled so that it contributed less to the overall variability than the between-animal differences. Nearly 5,000 photographic prints were prepared and measured to complete the processing of all 17 rats, and every precaution was taken to assure that the final estimates were reliable.

The 43% increase between 30 and 365 days (Fig. 2A) is surprisingly large. During this time, two aspects of granular layer morphology change, which together reflect the numerical increase. First, new neurons add to total granular layer volume (Fig. 2B). Second, ventral nuclear volume becomes smaller in older animals (Fig. 2C), which allows for increases in cell packing density. So older rats not only have a larger granular layer, but also tend to have more and smaller cells.

The absolute number of granule cells given here for 30 day Wistar rats is 42% above that reported by Schlessinger et al. (1975) for 28 day Holtzman rats. Genetic factors may be responsible for this difference, since Wimer et al. (1978) found granule cell numbers to vary as much as 60% between strains of mice. The range of values reported here for adults aged 120–200 days are similar to those reported by Gaarksjaer (1978) in Wistar rats weighing 200–300 g (0.99–1.19 million). On the other hand, these results cannot be easily related to the estimate of 2.17 million granule cells in adult Wistar rats (West and

Andersen 1980); the discrepancy is probably due to a major variation in estimation procedures. According to my understanding of the West and Andersen study, granule cell density measurements were taken from a set of animals prepared for electron microscopy, while total granular layer volume was measured in another set of animals. Thus, the final estimate was based on two different groups rather than on a complete analysis in several individual animals. This procedure could give inaccurate estimates, since the data in Fig. 2 show considerable variability between animals in a single age group. Still, if the data in Fig. 2A are extrapolated to approximately 2 years of age, they would approach the value obtained by West and Andersen; perhaps these investigators used older rats.

### *The Significance of the Data*

If  $^3\text{H}$ -thymidine injections are given between birth and postnatal day (P) 20 (survival to P60), approximately 85% of granule cells in the dentate gyrus are labeled (Bayer and Altman 1974; Bayer 1980). The  $^3\text{H}$ -thymidine autoradiographic analysis presented here shows that granule cells arise up to, and probably beyond, P180 in rodents, in agreement with several reports of granule cell labeling during adulthood (Altman 1963; Altman and Das 1965, 1966; Bayer 1976; Kaplan and Hinds 1977). In light of these data, the proportion of granule cells arising postnatally is continually enlarging. The earlier determination of 85% as the part of the population postnatally originating must now be regarded as a conservative estimate. The volumetric analysis shows that these new neurons add to the population, and this study marks the first demonstration of an increase in a neuronal population during adulthood in the mammalian brain.

In the rat, not only dentate granule cells, but also the granule cells in the cerebellum and olfactory bulb arise after birth. Virtually all of the cerebellar granule cells are generated between birth and 21 days of age (Altman 1969a). Although neurogenesis can be slightly prolonged by conditions of hypothyroidism (Nicholson and Altman 1972) and undernutrition (Barnes and Altman 1973), cerebellar granule cells are not produced during adult life. At least 70–80% of the main olfactory bulb granule cells originate postnatally (Altman 1969b; Bayer, in prep.), and neurogenesis continues during the adult period (Kaplan and Hinds 1977; Bayer, in prep.). However, a volumetric study of the total number of olfactory bulb granule cells reported no significant increases between 30 and 360 days of age (Roselli-Austin and

Altman 1979), implicating that as new neurons originate, mature ones die. Even though morphological evidence of hippocampal granule cell death, such as pyknotic fragments in the granular layer, is almost never observed, dentate granule cells may also be dying in adult rats. If so, the data of this study indicate that the rate of cell production exceeds the rate of cell death to bring about a net gain. Thus, the dentate granule cells may be the only one of the late-forming granule cell populations to increase during the adult period.

The volumetric analysis shows that granule cells are added at a constant rate (Fig. 2A), while the analysis of adult granule cell neurogenesis shows a sharp decline (Fig. 4) in the ratio of labeled cells to total cells when  $^3\text{H}$ -thymidine injections are begun at progressively later ages. Since the ratios in Fig. 4 were obtained at P200, one would expect a more constant level of labeled granule cells. However, there is a confounding factor that makes quantitative correlation between the volumetric and autoradiographic data difficult. At 200 days of age, few precursor cells and many granule cells are labeled when  $^3\text{H}$ -thymidine injections are given on days 60–63, while the reverse is true when injections are given on days 180–183. This is so because  $^3\text{H}$ -thymidine will only be incorporated by multiplying precursor cells, not by granule cells. Some of their progeny may remain precursors, while some others may differentiate into granule cells after an undetermined amount of time. The longer survival time of the earlier injection group allows for more granule cell production by labeled precursors than in the later injection group.

The gradients of neurogenesis in the adult granule cell population closely match those observed during the main period of granule cell origin (Bayer 1980). The septal and temporal extremes, especially the ectal limbs, have a low level of postnatal neurogenesis, and adult neurogenesis is almost nonexistent. The rest of the granular layer is mostly of postnatal origin and has prominent adult neurogenesis occurring throughout its extent. The slight gradient observed between ectal and endal limbs in the bulk of the granular layer (middle graph, Fig. 5) probably has minimal morphological and functional significance.

### Concluding Remarks

Assigning a specific function to the hippocampus is still controversial. Many experiments show it to be involved in short term memory (Scoville and Milner 1957; Hirsch 1974; Kapp et al. 1978), especially

spatial memory (O'Keefe and Nadel 1978; Olton 1978). Other studies implicate hippocampal activity in response inhibition (Douglas and Pribram 1966; Douglas 1967; McCleary 1966), which develops in synchrony with the maturation of the dentate gyrus (Altman et al. 1973; Douglas 1975). Whatever the function may be, dentate granule cells must play a pivotal role, since their elimination by early postnatal X-irradiation in rats gives behavioral deficits similar to those seen after bilateral hippocampal lesions (Bayer et al. 1973; Gazzara and Altman 1981). The continued increase of dentate granule cells in the adult suggest that their influence on total hippocampal function grows with age.

*Acknowledgements.* Excellent statistical consultation was provided by Dr. J.W. Yackel and Dr. P.S. Puri, Statistics Department, Purdue University. I also wish to thank Dr. Joseph Altman for advice and encouragement. Sharon Evander, Linda Ross, and Kim Sandefur provided the histology. Carol Landon did all photographic developing and printing. Martin Mucciarone wrote most of the computer programs. Teresina Chen, Carla Hoover, Jon Haux, and William Stumbo collected the computer data. Janet Dunn typed the manuscript.

### Appendix

#### *Detailed Procedures in Estimating the Total Number of Granule Cells*

*Dorsal-Ventral Parcellation.* Pilot studies showed average nuclear volume to be consistently larger in ventral than in the dorsal dentate granular layer of the hippocampus. In order to improve the accuracy of the final estimate, the number of granule cell nuclei was separately determined in ventral and dorsal parts. The part of the dentate gyrus lying posterolateral to the thalamus was designated as "ventral", while the part remaining lying either directly above or dorsolateral to the thalamus was designated as "dorsal". In slices where the granular layer was cut into anterior and posterior segments, the anterior part was "dorsal" while the posterior part was "ventral".

*Sampling Procedures.* In each animal, the analysis began with the preparation of low magnification photomicrographs (Fig. 1A, B) of the granular layer separated by 195  $\mu\text{m}$  in the ventral part, 39  $\mu\text{m}$  in the dorsal part. Within each of these slices, the granular layer was divided into 25  $\mu\text{m}$  wide strips running perpendicular to the length; each strip was considered to be a possible sample. Using a table of random numbers, 200 samples (n) were chosen from the total pool in all ventral and dorsal slices for examination. The proportion of ventral vs. dorsal strips selected for analysis reflected the relative numbers of samples available in the two parts of the granular layer. The number of strips selected in the *i*th slice was an integer (*n<sub>i</sub>*) approximated by:

$$(200) (N_i D_i S_i / \sum_{i=1}^k N_i D_i S_i),$$

where  $N_i$  is the total number of sample points available in the *i*th slice of *k* total slices,  $D_i$  is the distance to the next slice to be sampled, and  $S_i$  is an estimate of the variability. Pilot studies showed that variability was greater in dorsal than in ventral slices. Using a Summagraphics digitizer interfaced to a Wang 2200

computer, the locations of selected samples were marked on the low magnification pictures, and photomicrographs of these areas were prepared at high magnification ( $40 \times$  objective, Zeiss). Figure 1C, D show representative samples from ventral and dorsal parts of the granular layer. After the high magnification pictures were printed, the same regions were relocated in the microscopic field, and all complete and partial granule cell nuclear profiles were outlined; nuclear profiles of glial, endothelial, and polymorph cells were excluded.

*The Estimation of Total Granule Cell Nuclear Volume ( $V_t$ ).* To estimate total granule cell nuclear volume ( $V_t$ ) in the ventral part of the granular layer, for example, the area of the granular layer ( $A_g$ ) in each slice, areas of each selected sample ( $A_s$ ), and areas of all complete and partial granule cell nuclear profiles ( $A_n$ ) within the selected samples were measured with the digitizer. Both  $A_s$  and  $A_n$  are outlined in Fig. 1C–D. The total area of granule cell nuclei in each slice ( $A_i$ ) was approximated by:

$$A_i = (\Sigma A_n / \Sigma A_s) (A_g).$$

Finally,  $V_t$  was the summed products of  $A_i$  for each slice and the distance ( $D$ ) to the next slice:

$$V_t = A_{i1}D_1 + A_{i2}D_2 + \dots + A_{ii}D_i,$$

where  $i$  is the last slice to contain the ventral part of the granular layer; the same procedure was applied to all slices of the dorsal part.

Since the material consisted of three-dimensional slices, not two-dimensional sections,  $V_t$  was overestimated because the projected image of a nucleus obliterated any perikaryal material lying directly above or below it, a phenomenon called the Holmes effect (Weibel 1969; Elias et al. 1971). On the other hand  $V_t$  was underestimated since each sample contained fragments of nuclear material that were too thin to absorb sufficient stain to be recognized. Therefore, the following modified correction factor was applied to  $V_t$  which took both estimation errors into account.

$$\frac{1}{1 + \frac{3T}{4R} - (q^2 / 2R^3) (3R - q)},$$

where  $T$  = slice thickness,  $R$  = radius of an average nucleus in either the dorsal or ventral part of the granular layer,  $q$  = the thickness of a nuclear fragment which can no longer be detected. In the available material, a value of  $q = 1 \mu\text{m}$  fit best with the empirical data. For a derivation of this formula, see Puri and Yackel (1981).

*Error Bounds.* Bounds on error were determined for the final numerical estimate ( $N = V_t / V_a$ ) of the number of granule cells in each animal. The variance (VAR) in the ventral part of the granular layer, for example, is the summed products of:

$$\text{VAR} = A_{g1}^2 s_1^2 D_1^2 + A_{g2}^2 s_2^2 D_2^2 + \dots + A_{gi}^2 s_i^2 D_i^2,$$

where  $A_{g1}$  is the area of the granular layer in the most ventral slice,  $s_1$  is the standard deviation for the nuclear proportional areas of all samples in this slice,  $D_1$  is the distance to the next slice to be analyzed, and  $i$  is the last slice to contain the ventral part of the granular layer. In slices where only one sample was analyzed, the highest standard deviation found in any ventral slice was substituted. The 95% confidence interval for the numerical estimate in the ventral part ( $C_v$ ) was equal to:

$$C_v = \frac{2 \sqrt{\text{VAR}}}{V_a}.$$

The same procedure was followed for the calculation of VAR and the 95% confidence interval in the dorsal part ( $C_d$ ). Finally, the 95% confidence interval on the sum of ventral and dorsal granule cells ( $C_t$ ) was:

$$C_t = \sqrt{C_v^2 + C_d^2}.$$

## References

- Abercrombie M (1946) Estimation of nuclear population from microtome sections. *Anat Rec* 94: 239–247
- Altman J (1963) Autoradiographic study of cell proliferation in the brains of rats and cats. *Anat Rec* 145: 573–592
- Altman J (1969a) Autoradiographic and histological studies of postnatal neurogenesis. III. Dating the time of production and onset of differentiation of cerebellar microneurons in rats. *J Comp Neurol* 136: 269–294
- Altman J (1969b) Autoradiographic and histological studies of postnatal neurogenesis. IV. Cell proliferation and migration in the anterior forebrain, with special reference to persisting neurogenesis in the olfactory bulb. *J Comp Neurol* 137: 433–458
- Altman J, Das GD (1965) Autoradiographic and histological evidence of postnatal hippocampal neurogenesis in rats. *J Comp Neurol* 124: 319–336
- Altman J, Das GD (1966) Autoradiographic and histological studies of postnatal neurogenesis. I. A longitudinal investigation of the kinetics, migration and transformation of cells incorporating tritiated thymidine in neonate rats, with special reference to postnatal neurogenesis in some brain regions. *J Comp Neurol* 126: 337–390
- Altman J, Brunner R, Bayer SA (1973) The hippocampus and behavioral maturation. *Behav Biol* 8: 557–596
- Barnes D, Altman J (1973) Effects of two levels of gestational-lactational undernutrition on the postweaning growth of the rat cerebellum. *Exp Neurol* 38: 420–428
- Bayer SA (1976) Ontogeny of the hippocampal region in the rat. Paper presented at the Neurosciences Research Program Work Session on The Hippocampal Formation: Structure and Function. Woods Hole, MA, May 11–14, 1976
- Bayer SA (1980) The development of the hippocampal region in the rat. I. Neurogenesis examined with  $^3\text{H}$ -thymidine autoradiography. *J Comp Neurol* 190: 87–114
- Bayer SA, Altman J (1974) Hippocampal development in the rat: Cytogenesis and morphogenesis examined with autoradiography and low-level X-irradiation. *J Comp Neurol* 158: 55–80
- Bayer SA, Altman J (1975) Radiation-induced interference with postnatal hippocampal cytogenesis in rats and its long-term effects on the acquisition of neurons and glia. *J Comp Neurol* 163: 1–20
- Bayer SA, Brunner RL, Hine R, Altman J (1973) Behavioural effects of interference with the postnatal acquisition of hippocampal granule cells. *Nature* 242: 222–224
- Conover WJ (1971) Practical nonparametric statistics. Wiley, New York
- Douglas RJ (1967) The hippocampus and behavior. *Psychol Bull* 67: 416–422
- Douglas RJ (1975) The development of hippocampal function: Implications for theory and therapy. In: Isaacson RL, Pribram KH (eds) *The hippocampus: Neurophysiology and behavior*, vol 2. Plenum Press, New York, pp 327–361
- Douglas RJ, Pribram KH (1966) Learning and limbic lesions. *Neuropsychologia* 4: 197–220
- Elias H, Hennig A, Schwartz DE (1971) Stereology: Applications to biomedical research. *Phys Rev* 51: 158–200



- Gaarskjaer FB (1978) Organization of the mossy fiber system of the rat studied in extended hippocampi. I. Terminal area related to number of granule and pyramidal cells. *J Comp Neurol* 178: 49-72
- Gazzara RA, Altman J (1981) Early postnatal X-irradiation of the hippocampus and discrimination learning in adult rats. *J Comp Physiol Psychol* 95: 484-495
- Hendry IA (1976) A method to correct adequately for the change in neuronal size when estimating neuronal numbers after nerve growth factor treatment. *J Neurocytol* 5: 337-349
- Hirsch R (1974) The hippocampus and contextual retrieval of information from memory. *Behav Biol* 12: 421-444
- Kaplan MS, Hinds JW (1977) Neurogenesis in the adult rat: Electron microscopic analysis of light radioautographs. *Science* 197: 1092-1094
- Kapp BS, Gallagher M, Holmquist BK, Theall CL (1978) Retrograde amnesia and hippocampal stimulation: Dependence upon the nature of associations formed during conditioning. *Behav Biol* 24: 1-23
- McCleary RA (1966) Response-Modulation functions of the limbic system: Initiation and suppression. In: Stellar E, Sprague JN (eds) *Progress in physiological psychology*. Academic Press, New York, pp 209-272
- Nicholson JL, Altman J (1972) The effects of early hypo- and hyperthyroidism on the development of rat cerebellar cortex. I. Cell proliferation and differentiation. *Brain Res* 44: 13-23
- O'Keefe J, Nadel L (1978) *The hippocampus as a cognitive map*. Clarendon Press, Oxford, England
- Olton DS (1978) The function of septo-hippocampal connections in spatially organized behavior. In: *Functions of the septo-hippocampal system*. CIBA Foundation Symposium 58. Elsevier, Amsterdam, pp 327-342
- Puri PS, Yackel JW (1981) Statistical estimation of the number of spherical bodies embedded in a three-dimensional medium. Dept. of Statistics, Mimeo Series, Purdue University, West Lafayette, IN, USA
- Roselli-Austin L, Altman J (1979) The postnatal development of the main olfactory bulb of the rat. *J Dev Physiol* 1: 295-313
- Schlessinger AR, Cowan WM, Gottlieb DI (1975) An autoradiographic study of the time of origin and the pattern of granule cell migration in the dentate gyrus of the rat. *J Comp Neurol* 159: 149-176
- Scoville W, Milner B (1957) Loss of recent memory after bilateral hippocampal lesions. *J Neurol Neurosurg Psychiatry* 20: 11-21
- Weibel ER (1969) Stereological principles of mophometry in electron microscopic cytology. *Int Rev Cytol* 26: 235-302
- West MJ, Andersen AH (1980) An allometric study of the area dentata in the rat and mouse. *Brain Res Rev* 2: 317-348
- Wimer RE, Wimer CC, Vaughn JE, Barber RP, Balvanz BA, Chernow C (1978) The genetic organization of neuron number in the granule cell layer of the area dentata in house mice. *Brain Res* 157: 105-122

Received August 25, 1981